Resilience: nitrogen limitation, mycorrhiza and long-term palaeoecological plant-nutrient dynamics

Michael B. Bonsall(1)*, Cynthia A. Froyd(2), Elizabeth S. Jeffers(1)

(1) Mathematical Ecology Research Group, Department of Zoology,

University of Oxford, Oxford. OX1 3PS. U.K.

(2) Department of Biosciences, Swansea University, Swansea. SA2 8PP. U.K.

---

*Correspondence: Professor Michael B. Bonsall, Mathematical Ecology Research Group, Department of Zoology, University of Oxford, South Parks Road, Oxford. OX1 3PS. Tel. 01865 278916; email: michael.bonsall@zoo.ox.ac.uk

Abstract

Ecosystem dynamics are driven by both biotic and abiotic processes, and perturbations can push ecosystems into novel dynamical regimes. Plant-plant, plant-soil and mycorrhizal associations all affect plant ecosystem dynamics; however, the direction and magnitude of these effects vary by context and their contribution to ecosystem resilience over long time periods remains unknown. Here, using a mathematical framework, we investigate the effects of plant feedbacks and mycorrhiza on plant-nutrient interactions. We show evidence for strong nutrient controlled feedbacks, moderation by mycorrhiza and influence on ecological resilience. We use this model to investigate the resilience of a longitudinal paleoecological birch-δ^{15}N interaction to plant-soil feedbacks and mycorrhizal associations. The birch-δ^{15}N system demonstrated high levels of resilience. Mycorrhiza were predicted to increase resilience by supporting plant-nitrogen uptake and immobilizing excess nitrogen; in contrast, long-term enrichment in available nitrogen by plant-soil feedbacks is expected to decrease ecological resilience.

1 Introduction

Plants require soil nutrients for growth and actively influence nutrient cycles such as nitrogen. Such plant-soil feedbacks include the uptake and retention of nitrogen in plant tissues, release of nitrogen into leaf litter and woody debris, and support of ectomycorrhizal fungi (ECMs) that can influence plant access to multiple soil resources to support further plant growth. These plant-fungi associations have been shown to provide up to 80% of a plant's nitrogen requirements (Hobbie & Hobbie 2006) and thus play a fundamental role in promoting resilience of populations and ecosystem functioning; however, in some cases, ECMs compete with plants for resources by immobilizing nitrogen in mycelia (van der Heijden et al. 2015) and/or inhibiting plant access to nitrogen (Johnson et al. 1997), thus modulating the availability and mineralization of nitrogen (Näsholm et al. 1998) to support plant growth and potentially destabilizing plant-nitrogen interactions. Whether ECMs support or suppress plant growth depends on the abundance of host plant species, type of microbial associations, life cycle stage of the plant, nitrogen availability in the ecosystem and other environmental conditions (van der Heijden et al. 2015; Högberg et al. 2017). Furthermore, the relative importance of plant-plant interactions and plant-soil feedbacks in determining plant dynamics (Lekberg et al. 2018) and the potential mitigating effect of mycorrhiza (Mariotte et al. 2018) remains a contemporary research topic (e.g., Högberg et al. 2017). Such complexity challenges efforts to predict the stability and resilience of plant-nitrogen interactions over periods of environmental change. Palaeoecological proxy data on plant biomass and terrestrial nitrogen availability provide unique and valuable long-term observations required to assess the resilience of ecological interactions subject to environmental perturbations operating over centuries and/or millennia (Jeffers et al. 2015a).

Here, we hypothesise that mycorrhizal associations contribute to ecosystem resilience by modifying interactions between plants and available nutrients. We use a mathematical framework, built upon previous work (Jeffers et al. 2011, 2012, 2015b, 2018), to investigate the contribution of mycorrhiza to plant-nitrogen dynamics and ultimately ecological resilience. We then fit this model to a palaeoecological birch-nitrogen time series to assess the resilience of a natural system to alterations in plant-nutrient abundances and interactions with mycorrhiza.

2 Material and Methods

Mathematical Model

To investigate how the presence of mycorrhiza affect plant (P) - nitrogen (N) dynamics, and more broadly ecological resilience, we construct a mathematical model of plant and nitrogen dynamics. The model builds on those used to interrogate plant-nitrogen interactions from palaeoecological data (Jeffers et al. 2011, 2012, 2015). Population growth is dependent on available nitrogen and plants influence ecosystem-scale nitrogen availability through the release of decaying tissues. ECMs can affect plant growth by moderating nitrogen uptake and and/or competing for nitrogen (Högberg et al. 2017) immobilizing plant-available nitrogen (Näsholm et al. 2013). Mycorrhiza affect nitrogen loss rates from the system and/or help recycle organic forms of nitrogen that can be used by plants (Näsholm et al. 1998). Given this, we focus on the effects of ECMs on plant nitrogen uptake and immobilization. Our model framework is of the form:

$$\frac{dN}{dt} = \lambda - f(N,P) - j(N,M) - \mu_n N + g(P) \tag{1}$$

$$\frac{dP}{dt} = rf(N,P) - h(P)P - \mu_p P \tag{2}$$

where, in equation (1) describing the nutrient (N) dynamics, λ is the allochthonous input rate of nitrogen into the system, $f(N,P)$ is a function describing nitrogen uptake by plants (see below). $j(N,M)$ is the immobilization of nitrogen by mycorrhiza (M). This is not independent of other factors (such as carbon-nitrogen feedbacks or competition between mycorrhiza and other microbes) and to capture this breadth of outcomes we define $j(N,M) = \pm\gamma NM$, (where γ is the rate of immobilization). μ_n is the loss of nitrogen from the system through volatilization, dentrification or leaching, and $g(P)$ is a function describing the recycling of nitrogen from decaying plant biomass (see below).

In equation (2) describing the plant dynamics, r is the plant population growth rate, as noted above $f(N,P)$ is the uptake of nitrogen by the population for plant growth, $h(P)$ is a density-dependent plant feedback term ($h(P) = \nu P^{\beta}$) and μ_p is the (instantaneous) plant death rate.

Uptake rate. The uptake rate of nitrogen by plants is described by:

$$f(N,P) = (\alpha' NP) \tag{3}$$

where α' is the uptake coefficient describing the use of available nitrogen to support plant population growth. Nitrogen uptake is modulated by mycorrhiza according to $\alpha' = \alpha(1 + bM)$, where $b \in [-1, 1]$, such that mycorrhiza can behave mutualistically and increase (+) or parasitically and inhibit (-) plant access to sources of available nitrogen.

Nitrogen release rate. Nitrogen can be released back into the system as a function of plant biomass losses. We describe this process as a delayed response to plant biomass with:

$$g(P) = \mu_p \eta P(t - \tau) \tag{4}$$

where μ_p is the instantaneous death rate of the population, η is the proportion of plant biomass returned as available nitrogen and τ is the time lag between the release of plant biomass and transformation into available nitrogen. Given that nitrogen availability is structured through the soil profile (e.g., Högberg et al. 2017), this time delay captures the release of nitrogen from decaying plant biomass before it can be utilized by the plant or modulated by the mycorrhiza.

Analysis

The model analysis proceeds by addressing three questions (i) how does nitrogen uptake affect plant population growth, (ii) how do mycorrhiza moderate plant nitrogen uptake and ecosystem-scale nitrogen availability, and (iii) how is resilience of plant-nitrogen dynamics affected by plant-soil feedbacks, density-dependent population growth and modulation of soil resources by mycorrhiza. We use analytical (e.g., local stability analysis) and numerical (e.g., numerical integration) methods for model analysis (see supplementary information for fuller details). We then fit models to a long-term palaeoecological birch-δ^{15}N data set and assess ecological resilience.

3 Results

(i) Nutrient effects on plant dynamics

The effect of nitrogen uptake on plant population growth ($\frac{1}{P}\frac{dP}{dt}$) is estimated by:

$$\frac{1}{P}\frac{dP}{dt} = r[\alpha' N] - \nu P^{\beta} - \mu_p. \tag{5}$$

From this, positive plant population growth (fitness) occurs when $r[\alpha' N] > (\nu P^{\beta} + \mu_p)$. This inequality can be investigated further when plant populations are at equilibrial levels. This is $P^* = \left[\frac{r\alpha' N - \mu_p}{\nu}\right]^{(1/\beta)}$. At equilibrium, a baseline amount of nitrogen is required for positive plant population growth to occur (i.e. plant birth rate exceeds plant death rate). As mycorrhiza can act mutualistically (increase) or parasitically (inhibit) to affect plant nitrogen uptake ($\alpha' = \alpha(1 \pm M)$), this influences plant population growth.

Dynamics

To explore the specific mechanisms by which nitrogen availability affects plant dynamics, a limiting case of the full model can be derived.

If in the absence of plant density dependence, the nitrogen uptake rate exceeds background losses (e.g. by denitrification) and/or immobilization of nitrogen by mycorrhiza ($\alpha P >> (\mu_n + \gamma M)$), then the nitrogen-plant dynamics can be represented by:

$$\frac{dN}{dt} = \lambda - \alpha' NP + \mu_p \eta P(t-\tau) \tag{6}$$

$$\frac{dP}{dt} = r\alpha' NP - \mu_p P \tag{7}$$

If these nutrient dynamics act on a faster time scale than the plant dynamics then the steady state nutrient dynamics ($\overline{N}$) are:

$$\overline{N} = \frac{\lambda + \mu_p \eta P(t-\tau)}{\alpha' P}. \tag{8}$$

So the plant dynamics can then be approximated by:

$$\frac{dP}{dt} = r\left(\lambda + \mu_p \eta P(t-\tau)\right) - \mu_p P. \tag{9}$$

For small time delays $\tau \to 0$ then the solution to this expression for the plant dynamics at time T is:

$$P(T) = \frac{r\lambda}{\mu_p(r\eta - 1)}\left(\exp(t\mu_p(r\eta - 1)) - 1\right). \tag{10}$$

Provided $\eta < 1$ then the plant dynamics will asymptote and equilibriate at $\frac{r\lambda}{\mu_p(r\eta-1)}$. This equation shows that with greater allochthonous inputs of nitrogen (λ) or slower releases of nitrogen from decaying plant matter ($\mu_p(r\eta - 1)$), there will be a higher equilibrium plant population level ($P(T)$). This introduces nutrient-driven (*donor-controlled*) feedback mechanisms that can stabilize the plant dynamics.

For a given rate of external inputs of nitrogen (λ), the rate at which nitrogen is recycled from decaying plant biomass (η) has a strong effect on plant population dynamics (SI Fig. 1). High rates of release of plant-derived nitrogen destabilise the dynamics (leading to exponential plant population increases); increasing the background availability of nitrogen (λ) exacerbates the rate of this exponential increase (SI Fig. 1a). Lower rates of nitrogen release from decaying biomass stabilise plant population dynamics while increases in background supplies of nitrogen raise the realised equilibrium population level (SI Fig. 1b).

(ii) Mycorrhiza influence nutrient-plant dynamics

Given the plant-nutrient dynamics (eqns 1-2), the steady-state level of available nitrogen (N^*) is given:

$$N^* = \frac{\lambda + \mu_p\eta P^*}{\alpha' P^* + \gamma M + \mu_n}. \tag{11}$$

As might be expected, increases in uptake by plants ($\alpha' P^*$), immobilization by mycorrhiza (γM) or loss of nitrogen (μ_n) will all lead to lower steady-state levels of nitrogen. In contrast, increases in the allochthonous inputs of nitrogen (λ) and/or releases of nitrogen from decaying plant matter ($\mu_p\eta P^*$) will lead to higher steady-state levels of nitrogen.

Mutualistic mycorrhiza or parasitic mycorrhiza interact with plant-nutrient dynamics to affect levels of available nitrogen and nitrogen limitation of plant population growth (SI Fig. 2). In general, mutualistic mycorrhiza (when $\alpha' = \alpha(1 + M)$) favour stable plant-nutrient interactions (SI Fig. 2a). When mycorrhizae behave mutualistically, rising plant biomass and low levels of mycorrhizal biomass lead to asymptotic increases in available nitrogen. In contrast, parasitic mycorrhiza (when $\alpha' = \alpha(1 - M)$, reducing plant nitrogen uptake) can destabilize plant-nutrient dynamics (SI Fig. 2b). In this situation, increasing mycorrhizal biomass results in unregulated increases in available nitrogen (SI Fig. 2b) and destabilizes the dynamics (SI Fig. 3).

(iii) Effect of biotic feedbacks on resilience of plant-nitrogen interactions

To determine the resilience of the plant - nitrogen system we use a local stability analysis. We define resilience as the decay rate of perturbations back to the steady states and this rate is determined from the real part of the dominant eigenvalue associated with the local stability matrix (see SI). We use this approach to determine how resilience is affected by biotic feedbacks from plants and mycorrhiza.

The resilience of plant - nutrient dynamics is dependent on interactions with mutualistic mycorrhiza (when $\alpha' = \alpha(1 + M)$) (Figure 1). Increases in the proportion of plant biomass recycled as available nitrogen (η) decreases the resilience of the system (Fig. 1), such that any perturbation will grow over time, moving the system away from its current state. However this plant-soil feedback can be moderated by other biotic factors such as the rate of immobilisation (γ). At low levels of plant-nitrogen recycling, higher rates of immobilisation by mutualistic mycorrhiza leads to greater system resilience (Fig. 1a,c); however, there is a threshold point in the amount of plant-derived nitrogen beyond which increases in mycorrhizal immobilisation results in lower resilience.

Incorporating plant density-dependent plant dynamics ($h(P) = \nu P^{\beta}$) alters the shape of the resilience curve and the relative effect of immobilization at low levels of plant-derived nitrogen feedback (η) (Fig. 1c). Yet, the threshold point at which plant release rates lead to low resilience is the same for both the density-dependent and density independent models (Fig. 1c).

When mycorrhiza behave parasitically (when $\alpha' = \alpha(1 - M)$), the plant-nitrogen system is never resilient (i.e. resilience < 0) (Figs. 1b,d). In this situation, higher rates of mycorrhizal immobilization lead to lower system resilience in all circumstances.

(iv) Model-data comparison

To investigate the role of mycorrhiza on the resilience of plant-nutrient systems, we fit the model (eq 1-2) to a 5,000 year palaeoecological proxy time series of plant biomass (based on pollen accumulation rates) and nitrogen availability from Dubh Lochan (Great Glen, Scotland) (Froyd 2005; Jeffers et al. 2015b) using a Bayesian state space approach (see supplementary information). The series spans the early to mid-Holocene period (10,700 to 5,200 cal. yrs BP) and shows long-term declines in both birch and nitrogen availability after the first 2,000 years (see SI).

Comparing stochastic plant density-independent and density-dependent dynamic models to the data suggests that a plant density-independent model together with mutualistic mycorrhizal effects provides the most parsimonious description of the birch-nitrogen dynamics at Dubh Lochan (SI Fig. 4; $\chi^2_{\text{diff}} = 0.159$ on 2d.f., $p = 0.924$).

Using the parameterised density-independent plant-nutrient model (and observed relative abundances of birch and nitrogen), changes in predicted resilience of the plant-nutrient interaction at Dubh Lochan can be determined from the local stability matrix (used for the model analysis - see supplementary information). Figure 2 shows predicted resilience for the long-term birch-nitrogen system for four key parameters: rate of resource uptake (α), estimated mycorrhizal biomass (M), biomass release rate (η) and mycorrhizal immobilization rate (γ). Credible intervals from key posterior parameter distributions at each time point reveal how variation in parameters influences predicted resilience of the overall system. Increases in nutrient uptake rate (α) increase system resilience (i.e. small perturbations will decay away, Fig. 2a); however, increasing plant-derived available nitrogen (η) reduced resilience (i.e. any perturbation will grow over time, Fig. 2c). In general, greater biomass of mycorrhiza (M) further increases resilience (Fig. 2b). The predicted immobilisation rate (γ) varied over a narrow range of parameter values and the system remained resilient across all of them (Fig. 2d).

4 Discussion

Here, we have investigated the role of biotic interactions on the dynamics and resilience of plant-nutrient interactions. We show that nutrient-controlled (*donor-controlled*) feedbacks can determine plant population dynamics and equilibrium states (eq 9. & 10). How nutrients flow through the system, their availability and their immobilization determine plant population levels (SI Figs. 1a-b). Our model predictions show that high levels of plant-derived nitrogen enrichment can destabilize coupled plant-nitrogen dynamics. Immobilization of nitrogen by mycorrhizal associations can offset this effect (i.e. via the microbial bottleneck, sensu Knops et al. 2002) and improve resilience, but only at low levels of plant-derived nitrogen inputs. When nutrients increase beyond a threshold point, immobilization of nitrogen by mycorrhiza was predicted to reduced resilience. Similarly, direct interference in plant nitrogen uptake by mycorrhiza (i.e. parasitism) led to reduced resilience in all circumstances. Thus biotic interactions can strongly influence nutrient cycling (Chapman et al. 2006) and plant performance (Lekberg et al. 2018) by dampening or exacerbating feedback effects.

How important are these processes in real ecosystems? Our model-data comparison with palaeoecological birch-δ^{15}N data showed evidence for donor-controlled plant-nitrogen dynamics and mutualistic interactions with mycorrhizal fungi. Increasing plant nitrogen uptake had a positive effect on system resilience (Fig. 2a). Mycorrhiza were also associated with greater resilience (Fig. 2b), likely by promoting and regulating access to alternative available nitrogen sources (e.g., Read 1983). Our results conform with observations from modern ecosystems that although mycorrhizae have the potential to behave parasitically, mutualistic behaviour is more likely (Frederickson 2017), especially in nitrogen poor environments (Deckmyn et al. 2014).

Predicted immobilization rates, like mycorrhizal biomass, varied over a narrow range of values and - contrary to our model results - always led to greater system resilience (Fig. 2d). ECMs can immobilize nitrogen in relatively recalcitrant hyphae, which become part of the soil organic matter after they die, thus promoting nitrogen retention and regulating the rate of recycling of organic nitrogen (Deckmyn et al. 2014). This mechanism is predicted to improve resilience of birch-nitrogen interactions, likely by offsetting the negative effects of plant-driven feedbacks (Fig. 2c). That nitrogen immobilization has a prevalent role in birch-ECM dominated forests and plant dynamics are heavily influenced by nitrogen-carbon-microbe interactions (Högberg et al. 2017) highlights that alternative sources of (organic) nitrogen (e.g., amino acids - Read 1983) may be highly influential in these ecosystem dynamics (Näsholm et al. 1998). Together with long paleo-ecological records, the dynamics of ECMs and the sources of nitrogen availability in forest ecosystem resilience warrants much more in-depth scrutiny.

This is - to our knowledge - the first attempt to incorporate the role of mycorrhizal association into a plant-nitrogen dynamic model fitted to long-term palaeoecological data and used to assess ecosystem resilience. The results support the important role of biotic controls in nutrient cycling (e.g., Näsholm et al. 1998; Jeffers et al. 2011) and driving ecosystem resilience. A key limitation however is the current lack of continuous palaeoecological records of mycorrhizal biomass concurrent with other proxies (Strullu-Derrien et al. 2018). Future work should focus on linking carbon-nitrogen-microbe dynamics to plant-nutrient interactions, dynamics and resilience. These caveats notwithstanding we show that knowledge of the type, direction and magnitude of biotic interactions is critically important in determining the dynamics, stability and resilience of these ecological systems.

References

Chapman, S.K., Langley, J.A., Hart, S.C. G.W. Koch (2006) Plants actively control nitrogen cycling: uncorking the microbial bottleneck. New Phytologist, 169, 27-34. doi: 10.1111/j.1469-8137.2005.01571.x

Deckmyn, G., A. Meyer, M.M. Smits, A. Ekbald, T. Grebenc, A. Komarov and H. Kraigher (2014) Simulating ectomycorrhizal fungi and their role in carbon and nitrogen cycling in forest ecosystems. Canadian Journal of Forest Research, 44, 535-553. doi: 10.1139/cjfr-2013-0496

Frederickson, M.E. (2017) Mutualisms are not on the verge of breakdown. Trends in Ecology and Evolution, 32(10): 727-734. doi: 10.1016/j.tree.2017.07.001

Froyd, C.A. (2005) Fossil stomata, reveal early pine presence in Scotland: implications for postglacial colonization analyses. Ecology, 86, 579–586. doi: 10.1890/04-0546

Hobbie, E., and Hobbie, J. 2006. 15N in symbiotic fungi and plants estimates nitrogen and carbon flux rates in Arctic tundra. Ecology, 87(4): 816 – 822. doi:10.1890/0012-9658(2006)87[816:NISFAP]2.0.CO;2

Högberg, P., T. Näsholm, O. Franklin and M.N. Högberg (2017) Tamm review: on the nature of the nitrogen limitation to plant growth in Fennoscandian boreal forest. Forest Ecology and Management, 403: 161 - 185. doi: 10.1016/j.foreco.2017.04.045

Jeffers, E.S., M.B. Bonsall and K.J. Willis (2011) Stability in ecosystem functioning across a climatic threshold and contrasting forest regimes. PLoS ONE, 6(1), e16134. doi: 10.1371/journal.pone.0016134

Jeffers, E.S., M.B. Bonsall, J. Watson and K.J. Willis (2012) Climate change impacts on ecosystem functioning: evidence from an Empetrum heathland. New Phytologist 193 (1): 150-164. doi: 10.1111/j.1469-8137.2011.03907.x

Jeffers, E.S., S. Nogue and K.J. Willis (2015a) The role of palaeoecological records in assessing ecosystem services. Quaternary Science Reviews 112: 17-32. doi: 10.1016/j.quascirev.2014.12.018

Jeffers, E.S., M.B. Bonsall, C.A. Froyd, S.J. Brooks and K.J. Willis (2015b) The relative importance of biotic and abiotic processes for structuring plant communities through time. Journal of Ecology, 103, 459–472. doi: 10.1111/1365-2745.12365

Jeffers, E.S, N.J. Whitehouse, A. Lister, G. Plunkett, P. Barratt, E. Smyth, P. Lamb, M.W. Dee, S.J. Brooks, K.J. Willis, C.A. Froyd, J.E. Watson and M.B. Bonsall (2018) Plant controls on Late Quaternary whole ecosystem structure and function. Ecology Letters, 21, 814-825. doi: 10.1111/ele.12944

Johnson, N.C., J.H. Graham and F.A. Smith (1997) Functioning of mycorrhizal associations along the mutualism–parasitism continuum. New Phytologist, 135, 575-585. doi: 10.1046/j.1469-8137.1997.00729.x

Knops JMH, Bradley KL, Wedin DA. 2002. Mechanisms of plant species impacts on ecosystem nitrogen cycling. Ecology Letters 5: 454–466. doi: 10.1046/j.1461-0248.2002.00332.x

Lekberg,Y., J.D. Bever, R.A. Bunn, R,M, Callaway, M.M. Hart, S.N. Kivlin, J. Klironomos, B.G. Larkin, J.L. Maron, K.O. Reinhart, M. Remke, W.H. van Der Putten 2018 Relative importance of competition and plant–soil feedback, their synergy, context dependency and implications for coexistence. Ecology Letters, 21, 1268-1281. doi: 10.1111/ele.13093

Mariotte, P., Z. Mehrabi, T.M. Bezemer, G.B. de Deyn, A. Kulmatiski, B. Drigo, G.F.C. Veen, M.G.A. van der Heijden, P. Kardol (2018) Plant-Soil Feedback: Bridging Natural and Agricultural Sciences. Trends in Ecology and Evolution, 32: 129-142. doi: 10.1016/j.tree.2017.11.005

Näsholm, T., A. Ekblad, A. Nordin, R. Giesler, M. Hógberg and P. Högberg (1998) Boreal forest plants take up organic nitrogen. Nature, 392: 914-916. doi: 10.1038/31921

Näsholm, T., P. Högberg, O. Franklin, D. Metcalfe, S.G. Keel, C. Campbell, V. Hurry, S. Linder and M.N. H oberg (2013) Are ectomycorrhizal fungi alleviating or aggravating nitrogen limiation of tree growth in boreal forests? New Phytologist, 198: 214-221. doi: 10.1111/nph.12139

Read, D.J. (1983) The biology of mycorrhiza in the Ericales. Canadian Journal of Botany, 61: 985-1004. doi: 10.1139/b83-107

Strullu-Derrien, C., M.-A. Selosse, P. Kenrick, F.M. Martin (2018) The origin and evolution of mycorrhizal symbioses: from palaeomycology to phylogenomics. New Phytologist, 220, 1012-1030. doi: 10.1111/nph.15076

van der Heijden MG, Martin FM, Selosse MA, Sanders IR (2015) Mycorrhizal ecology and evolution: the past, the present, and the future. New Phytologist 205 (4) 1406-1423. doi: 10.1111/nph.13288

Bonsall MB, Froyd CA, Jeffers EM 2019 Data for: Resilience: nitrogen limitation, mycorrhiza and long-term palaeoecological plant-nutrient dynamics. Open Science Framework (http://osf.io/4mvba/)

Acknowledgements

We thank the reviewers and editors for their constructive comments on this work. Radiocarbon dates were provided by NERC Scientific Services, allocation number 787.0599

Figure Legends

Figure 1 – Resilience (decay rate of perturbations, see supplementary information) of plant – nutrient system to interactions with mycorrhiza under (A-B) density-independent or (C-D) density-dependent plant dynamics. With mutualistic mycorrhiza (A,C) increases in the rate at which plant biomass releases nitrogen can destablise the system and decreases resilience. Changes in the rate of immobilization (blue line to orange line to green line) on resilience depends on the plant population dynamics and biotic interactions. Parasitic mycorrhiza (B,D) always destabilize and make plant-nutrient systems less resilient.

Figure 2 - Predicted resilience of the birch-nitrogen system at Dubh Lochan for a range of model parameter values: (A) the predicted plant nutrient uptake rate (α), (B) the predicted mycorrhizal biomass (M), (C) the plant biomass release rate (η) and (D) the mycorrhizal nutrient immobilisation rate (γ). Parameter estimates are updated through time using a sequential Monte Carlo approach. Grey bars represent parameter credible intervals (estimated from the Bayesian state space) at a particular time point. Black bars are the range of predicted resilience levels (for a parameter at a particular time point).

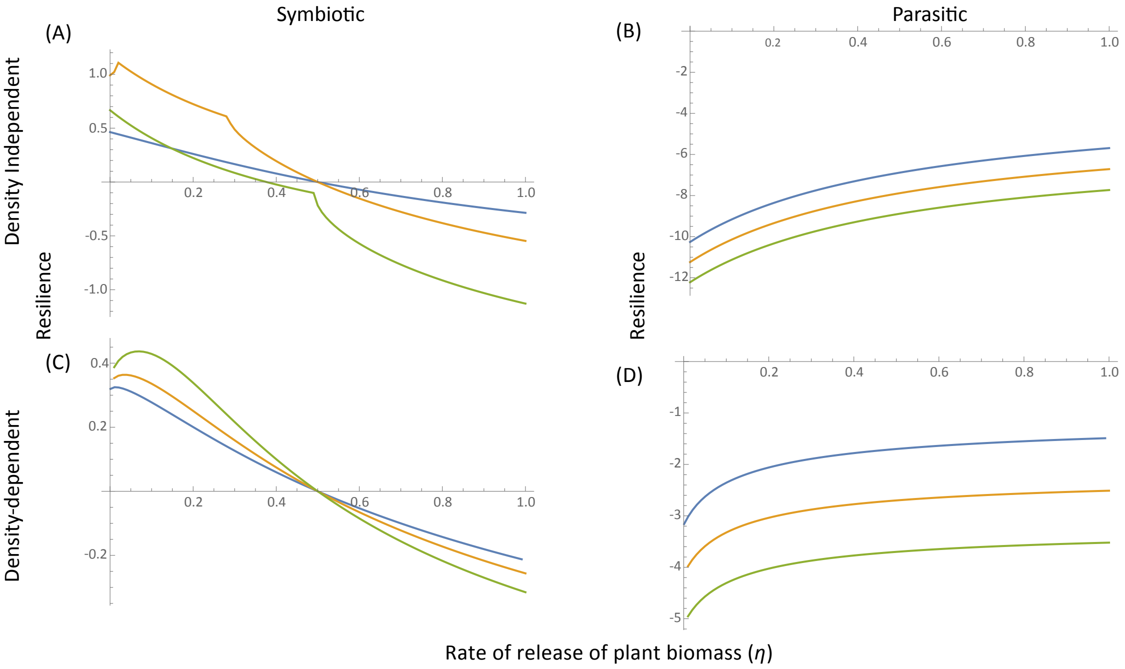
Symbiotic
Parasitic
(A)
(B)
(C)
(D)
Density Independent
Density-dependent
Resilience
Resilience
1.0
0.5
-0.5
-1.0
0.2
0.4
0.6
0.8
1.0
-2
-4
-6
-8
-10
-12
0.4
0.2
-0.2
-1
-2
-3
-4
-5
Rate of release of plant biomass (η)

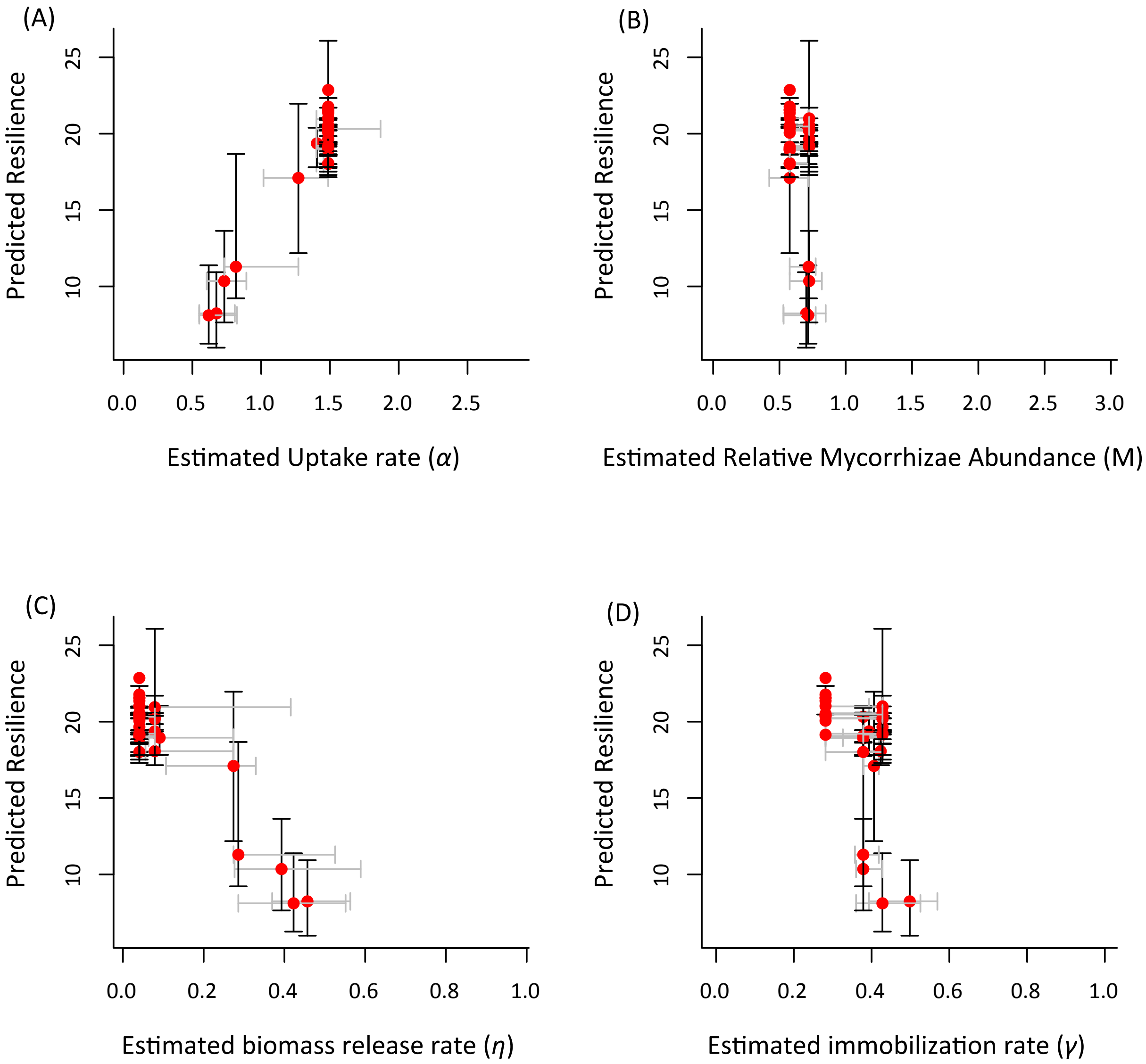
(A)
Predicted Resilience
10
15
20
25
0.0
0.5
1.0
1.5
2.0
2.5
Estimated Uptake rate (α)
(B)
Predicted Resilience
10
15
20
25
0.0
0.5
1.0
1.5
2.0
2.5
3.0
Estimated Relative Mycorrhizae Abundance (M)
(C)
Predicted Resilience
10
15
20
25
0.0
0.2
0.4
0.6
0.8
1.0
Estimated biomass release rate (η)
(D)
Predicted Resilience
10
15
20
25
0.0
0.2
0.4
0.6
0.8
1.0
Estimated immobilization rate (γ)

Supplementary Information

The sections in the supplementary information give further details on (i) dynamics, stability and resilience analysis of the plant-nutrient model, (ii) the palaeoecological data set and (iii) the Bayesian methods used to fit the models to the data set.

Dynamics, Stability and Resilience

The availability of nutrients has a strong effect on plant dynamics. Release of nutrients from the decaying plants can stabilize or destabilize dynamics (Fig. S1).

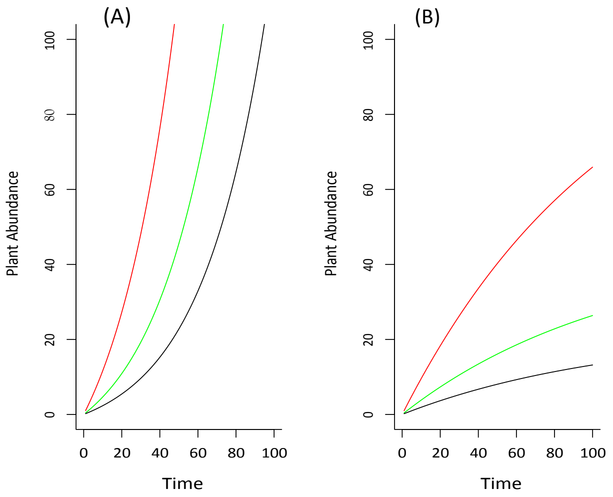

Figure S1. Effects of nitrogen availability on plant dynamics under (A) high and (B) low levels of nitrogen releases from plant biomass. High levels of nitrogen releases destabilize dynamics and increases in background nitrogen availability (λ > black to green to red) further exacerbate these unstable dynamics. Low levels of nitrogen releases from plant biomass promote stable plant dynamics and equilibrium levels increases as nitrogen availability increases.

Mycorrhizal associations interact with the plant nutrient dynamics to affect plant population-growth rate (Fig. S2) and the stability of the plant-nutrient system (Fig S3).

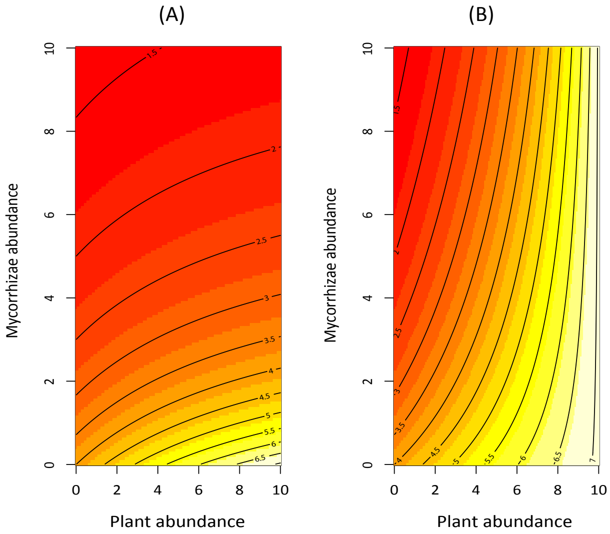

Figure S2. Effect of mycorrhizae association on nutrient dynamics and availability. Under (A) symbiotic mycorrhizal associations, low levels of mycorrhizal abundance and increasing plant biomass favour increases in nitrogen availability. In contrast, under (B) parasitic associations, increases in plant biomass and high mycorrhizae abundances favour increased nitrogen availability.

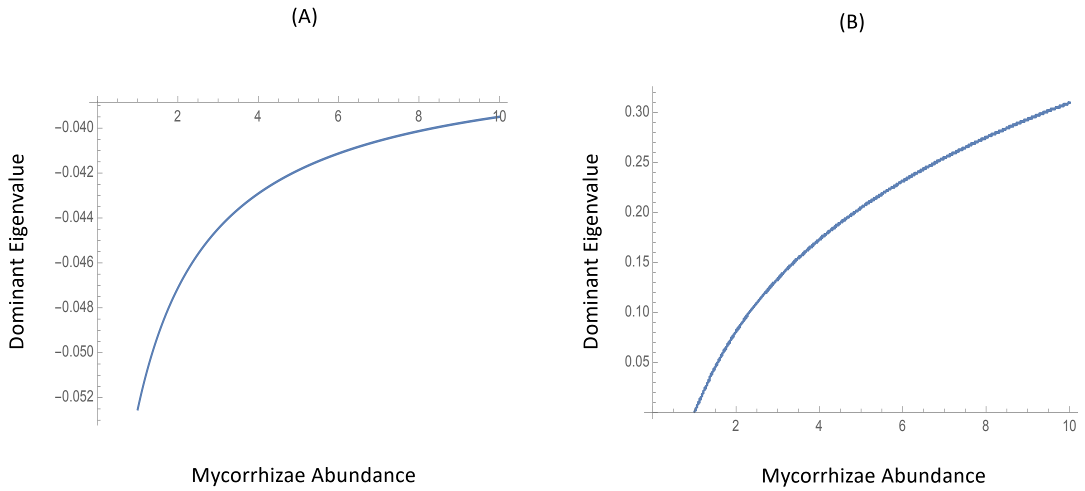

Figure S3 - Influence of mycorrhizal abundance on the stability of the plant-nutrient system under (A) symbiotic and (B) parasitic mycorrhizae. Symbiotic mycorrhizae give rise to stable plant-nutrient interaction (real part of the dominant eigenvalue is negative) whereas parasitic mycorrhizae destabilize the interaction (real part of the dominant eigenvalue is positive).

Resilience of the system is determined from the sign and magnitude of the dominant eigenvalue of the linearized dynamical system around an equilibrium state (e.g. Holling 1973; May 1973).

From the main text equations (1 & 2), the equilibrium states of the system (N^* and P^*) can be determined. In the absence of plant density dependence ($\nu \to 0$) the equilibria are:

$$N^* = \frac{\mu_p}{r\alpha'} \tag{A.1}$$

$$P^* = -\frac{\frac{\mu_p}{r\alpha'}\left(\gamma M - \mu_n\right) + \lambda}{\mu_p \eta + \frac{\mu_p}{r}}. \tag{A.2}$$

In the presence of density dependence ($h(P) = \nu P^{\beta}$ where β represent the strength of density-dependence, $\beta = 1$), the equilibria are:

$$N^* = \frac{\nu P^* + \mu_p}{r\alpha'}. \tag{A.3}$$

The solution for P^* under this form of density dependence is found from solving the following quadratic:

$$\frac{\nu P^* + \mu_p}{r\alpha'}\left(\alpha' P^* - \gamma M - \mu_n\right) - \lambda - \mu_p \eta P^* = 0. \tag{A.4}$$

Stability matrix

When $\beta = 1$ from main text equations (1-2):

$$\mathbf{J} = \begin{bmatrix} -\omega - \alpha' P^* + \gamma M - \mu_n & -\alpha' N^* + \mu_p \eta exp(-\omega\tau) \\ r\alpha' P^* & -\omega + r\alpha' N^* - 2\nu P^* - \mu_p \end{bmatrix}. \tag{A.5}$$

From the determinant of this matrix, the characteristic equation (when $exp(-\omega\tau \approx 1 - \omega\tau)$ is:

$$\omega^2 + \omega(A + D + B\mu_p\eta\tau) + B(C - \mu_p\eta) = 0 \tag{A.6}$$

where $A = \alpha' P^* - \gamma M - \mu_n$, $B = r\alpha' P^*$, $C = \alpha' N^*$ and $D = 2\nu P^* + \mu_p - r\alpha' N^*$ and the eigenvalues are found from:

$$\omega = -\frac{1}{2}\left(A + D + B\mu_p\eta\tau\right) \pm \sqrt{\left(A + D + B\mu_p\eta\tau\right)^2 - 4\left(B(C - \mu_p\eta)\right)}. \tag{A.7}$$

From Routh-Hurwitz criteria, stability of the interaction is ensured if $(A+D+B\mu_p\eta\tau) > 0$ and $B(C-\mu_p\eta) > 0$. Mutualistic mycorrhiza stabilize while parasitic mycorrhiza destabilize the plant-nutrient interaction (Fig. S3). Asymptotic resilience is the decay rate of perturbations in the linearized system and is determined from the real part of the dominant eigenvalue (ω) associated with this local stability matrix ($-\Re[\lambda_1(\mathbf{J})]$). The larger the resilience, the faster perturbations eventually decay to return the system to the steady state (Holling 1973).

Data set

Palaeoecological proxy data of plant biomass and available nitrogen were previously reconstructed from fossil pollen (Fig. S4a) and stable nitrogen isotope (Fig. S4b) analysis of lake sediments obtained from Dubh-Lochan in the Great Glen regions of the Scottish Highlands (Froyd 2005; Jeffers et al 2015). Here we use the chronology and pollen accumulation rates of birch reported in Jeffers et al. (2015).

Model Fitting Approaches: Bayesian State Space

We use a Bayesian hierarchical state-space approach to fit models to palaeoecological birch-N plant-nutrient data to account for uncertainties operating at different levels in the data. A data model links the observed proxy abundance measures for birch and N to an expected abundance measure (generated by a stochastic version of plant-nutrient dynamics - main text equations 1-2):

$$dN = [\lambda - f(N(t), P(t)) - j(N(t), M) - \mu_n N(t) + g(P(t))]\, dt + f(\sigma_n, N(t)) dW \tag{A.8}$$

$$dP = [r f(N(t), P(t)) - h(P)P - \mu_p P(t)]\, dt + f(\sigma_p, P(t)) dW \tag{A.9}$$

where $f(\sigma_n, N(t))$ and $f(\sigma_p, P(t))$ represents demographic error processes acting on nutrients and plants, respectively, and dW is a Brownian motion process. All other parameters are defined in the main text. We assume that measurement error can be assessed through a least-squares difference ($L(t)$) between the observed and (stochastic) expected abundances at each time point (t):

$$L(t) = \sum_{i=1}^{2} (O_i(t) - E_{is}(t))^2$$

where $O_i(t)$ is the observed abundance and $E_{is}(t)$ is the expected abundance (generated from the stochastic model) for the i^{th} proxy (birch or δ^{15}N) at time t.

The stochastic model (eqns A.8-A.9) describes the nonlinear ecological processes that underpin the plant-nutrient dynamics. For the palaeoecological birch-δ^{15}N data set, we compare two models: a plant-plant intraspecific density dependence model (where $h(P) = P^{\beta}$) and a plant density independent model (where $h(P) = 0$). Unknown (hidden) model parameters are assumed to be random variables and have either Gamma and/or Uniform priors. The error terms (σ_p, σ_n) are also assumed to be random variables and have Uniform priors. To account for additional process error in our hierarchical framework, we use a second least squares difference (L_{sd}) between the stochastic and deterministic version of the model:

$$L_{sd}(t) = \sum_{i=1}^{2} (E_{is}(t) - E_{id}(t))^2$$

where E_{id} is the expected abundance of the i^{th} proxy from numerically integration of the deterministic plant-nutrient dynamics.

To implement this Bayesian hierarchical state-space approach, we use a sequential Monte Carlo (SMC) algorithm, coupled with a standard Markov Chain Monte Carlo (MCMC) update step. These SMC approaches provide a general framework for dynamic state-space estimation (building on linear Kalman Filter methods) (e.g. Doucet et al. 2001; Cappé et al. 2007). In SMC approaches, a distribution of interest (e.g. for a parameter) is approximated by a large set of random samples ('particles'). The trajectories of these particles are propagated using a recursive importance sampling/resampling scheme. Beginning with an initial distribution the posterior density (e.g., for a parameter) can be obtained by samples Q trajectories from an importance distribution and computing a set of weights.

The *bootstrap filter* (Gordon et al. 1993) provides a robust sampling distribution (which in our case is based on a least squares difference: $g(\mathbf{O}(t), \mathbf{E_s}(t) = \sum_{i=1}^{2} L_i(t))$ - where $\mathbf{O}(t)$ is the vector of observations and $\mathbf{E_s}(t)$ is the vector of expected abundances from numerical integration of the stochastic model (eqns: A.8-A.9) at time t). For a large number of particles ($k = 1, \ldots, Q$), the normalised importance weights for each particle is:

$$w_k = \frac{\sum_{i=1}^{2} L_i^k}{\sum_{j=1}^{Q} \sum_{i=1}^{2} L_i^j}.$$

However, one limitation of these sequential importance sampling methods is that the weights can become highly degenerate such that the probability mass is concentrated onto a very small proportion of particles/weights (such that most particles contribute very little to the expectation estimations). To avoid this potential problem, several solutions have been proposed (e.g. Cappé et al. 2007) that involve some form of (re)sampling of particles with replacement (which we implement in our algorithms).

Parameter estimation implements a standard MCMC step (Gilks & Berzuini 2001; Bonsall et al. 2014). Under this scheme the bootstrap filter is extended to (i) resample particles with probabilities proportional to their weights and (ii) implement a MCMC move (or moves) on each particle. Here, we implement a Metropolis-Hastings MCMC within the bootstrap filter to derive expectation estimates (for a vector of parameter $\mathbf{H}$) up to time point T. Parameter estimates are updated sequentially as the time series evolves and data at additional census points become available. As such our MCMC sampling follows:

$$\phi(T) = \frac{g(\mathbf{O}(t), \mathbf{E_s^*}(t))g(\mathbf{E_s^*}(t), \mathbf{E_d^*}(t))f(\mathbf{H}^*(t))f(\sigma_p^*)f(\sigma_n^*)}{g(\mathbf{O}(t), \mathbf{E_s}(t))g(\mathbf{E_s}(t), \mathbf{E_d}(t))f(\mathbf{H}(t))f(\sigma_p)f(\sigma_n)}$$

where $\mathbf{E_s}(t)$ and $\mathbf{E_d}(t)$ are expected values from the stochastic model and deterministic plant-nutrient model, respectively. $g(\cdot, \cdot)$ denotes a least-squares difference and $f(\cdot)$ a prior. The proposal distribution, denoted by *, follows a Normal distribution with a fixed variance to determine a feasible acceptance rate. Computationally, we implement this hierarchical model in R (R Core Team 2013) and use a log-scale to determine $min(0, log(\phi))$ and set $\mathbf{H}(t) = \mathbf{H}^*(t)$ with probability X and $\mathbf{H}(t) = \mathbf{H}(t)$ with probability $1 - X$.

Goodness of Fit

To evaluate goodness of fit, we used one-step ahead predictions (Fig. S4) and evaluated the difference between the observations and expected values (based on posterior parameter modes) using χ^2 test. Expected parameter distributions (and parameter points estimates based on posterior modes) are used to determine predicted resilience for the most parsimonious model. Credible intervals are used to determine parameter uncertainty and hence resilience uncertainty across the dynamics of the palaeoecological birch-δ^{15}N time series.

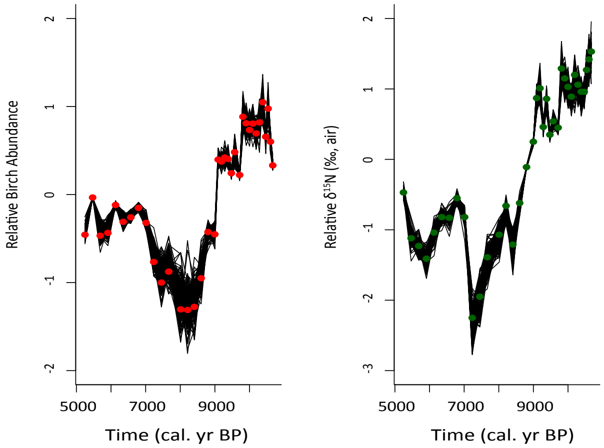

Figure S4. One step ahead predictions for the (A) birch and (B) nitrogen dynamics from Dubh Lochan. Relative birch and nitrogen observed abundance (solid points) together with realizations from the stochastic plant-nutrient model (black lines) used in the Bayesian state space fitting. Stochastic realizations are characterized by evolving parameter values as the time series unfolds and the model fit highlights a plant density independent model where donor controlled dynamics coupled to symbiotic mycorrhizae best described the birch and nitrogen dynamics at Dubh Lochan.

Model Calibration

To validate the accuracy of the resampling algorithm and ensure that the methods avoid particle depletion, we simulated plant-nutrient dynamics using the following baseline model:

$$\frac{dN}{dt} = \lambda - \alpha NP - \mu_n N + \eta \mu_p P \tag{A.10}$$

$$\frac{dP}{dt} = \alpha NP - \mu_p P \tag{A.11}$$

where λ is the allochthonous input rate of nitrogen into the system, μ_n is the loss of nitrogen from the system, μ_p is the (instantaneous) plant death rate, α' is the uptake coefficient describing the use of available nitrogen to support plant population growth and η is the proportion of plant biomass returned as available nitrogen. With fixed parameter values, $\lambda = 4.0$, $\alpha = 0.005$, $\eta = 0.001$, $\mu_n = 0.1$ and $\mu_p = 0.1$, stochastic plant-nutrient dynamics were simulated with the Gillespie algorithm (Gillespie, 1976, 1977) . Representative illustration of the dynamics for the plant-nutrient system are shown in Fig. S5.

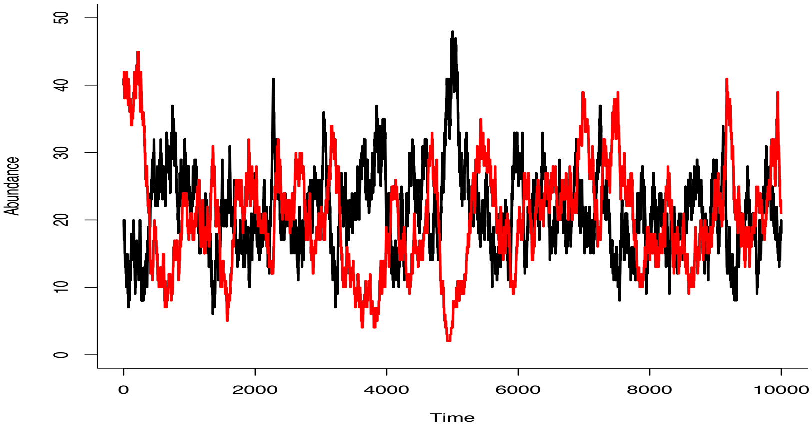

Figure S5 – Simulated plant (red line) – nutrient (black line) dynamics (using Gillespie algorithm from equations A.10-A.11 with fixed parameter values (λ=4.0, α=0.005, η=0.001, μ_n=0.1 and μ_p=0.1)

To evaluate the potential bias introduced by the resampling approach, we fit the stochastic model:

$$dN = [\lambda - \alpha NP - \mu_n N + \eta P)]\, dt + f(\sigma_n, N)dW \tag{A.12}$$

$$dP = [\alpha NP - \mu_p P]\, dt + f(\sigma_p, P)dW \tag{A.13}$$

where σ_n and σ_p are noise terms for the nutrient and plant dynamics, respectively, with 250 particles in the sequential Monte Carlo sampler. Our resampling algorithm is robust to issues of particle degeneracy with the probability mass of the posterior distributions generally centred around the known parameter values (Fig. S6) for our simulated data.

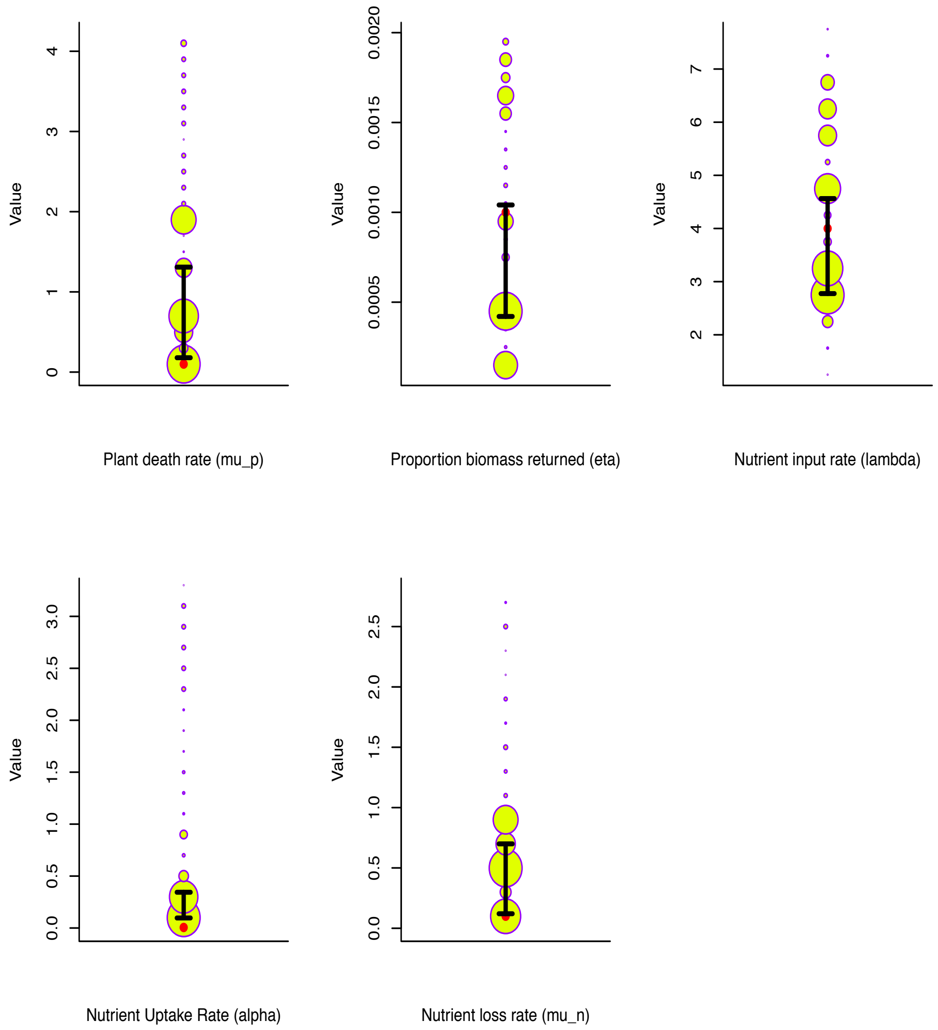

Figure S6 - Posterior distributions for the parameters values for the plant-nutrient dynamics from simulated data. The diameter of the circles represent the probability mass for parameter values within the posterior distribution, the black bar is the interquartile credible intervals and the red point is the true (fixed) parameter value.

References

Bonsall, M.B., C.A. Dooley, A. Kasparson, T. Brereton, D.B. Roy and J.A. Thomas (2014) Allee effects and the spatial dynamics of a locally endangered butterfly, the high brown fritillary (Argynnis adippe). Ecological Applications, 24, 108-120. doi: 10.1890/13-0155.1

Cappé, O., S.J. Godsill and E. Moulines (2007) An overview of existing methods and recent advances in sequential monte carlo. Proceedings of the IEEE, 95, 889–924. doi: 10.1109/JPROC.2007.893250

Doucet, A., N. de Freitas, and N. Gordon (2001) Sequential Monte Carlo methods in practice. Springer, Berlin.

Froyd, C.A. (2005) Fossil stomata, reveal early pine presence in Scotland: implications for postglacial colonization analyses. Ecology, 86, 579–586. doi: 10.1890/04-0546

Gillespie, D.T. (1976) A general method for numerically simulating the stochastic time evolution of coupled chemical reactions. Journal of Computational Physics, 22, 403–434. doi:10.1016/0021-9991(76)90041-3.

Gillespie, D.T. (1977) Exact stochastic simulation of coupled chemical reactions. Journal of Physical Chemistry, 81, 2340–2361. doi:10.1021/j100540a008.

Gilks, W.R. and C. Berzuini (2001) Following a moving target - Monte Carlo inference for dynamic Bayesian models. Journal of the Royal Statistical Society, Series B, 63, 127–146. doi: 10.1111/1467-9868.00280

Gordon, N.J., D.J. Salmond, and A.F.M. Smith (1993) Novel approach to nonlinear non-Gaussian Bayesian state estimation. IEE Proceedings F, 140, 107–113. doi: 10.1049/ip-f-2.1993.0015

Holling, C.S. (1973) Resilience and stability of ecological systems. Annual Review of Ecology and Systematics, 4, 1-23. doi: 10.1146/annurev.es.04.110173.000245

Jeffers, E.S., M.B. Bonsall, C.A. Froyd, S.J. Brooks and K.J. Willis (2015) The relative importance of biotic and abiotic processes for structuring plant communities through time. Journal of Ecology, 103, 459–472. doi: 10.1111/1365-2745.12365

May, R.M. (1973) Stability and complexity in model ecosystems. Princeton University Press, Princeton.

R Core Team (2013). R: A language and environment for statistical computing. R Foundation for Statistical Computing, Vienna, Austria. URL http://www.R-project.org/.